RSC Publishing JAAS

XAS study of Mn, Fe and Cu as indicators of historical glass decay

Journal:	*Journal of Analytical Atomic Spectrometry*
Manuscript ID:	Draft
Article Type:	Paper
Date Submitted by the Author:	n/a

Complete List of Authors:	Abuin, Manuel; Complutense University of Madrid, Materials Physics Serrano, Aida; Glass and Ceramic Institute, CSIC Chaboy, Jesus; Instituto de Ciencia de Materiales de Aragon, Solid State Physics Garcia, Miguel-Aanguel; Glass and Ceramic Institute, CSIC Carmona, Noemi; Complutense University of Madrid, Materials Physics

XAS study of Mn, Fe and Cu as indicators of historical glass decay

M. Abuín[1], A. Serrano[2], J. Chaboy[3], M.A. García[2,4], N. Carmona[1]

[1] Department of Materials Physics, Complutense University at Madrid, Avda. Complutense sn, 28004 Madrid, Spain

[2] Glass and Ceramic Institute, CSIC, C. Kelsen 5, 28049 Madrid, Spain

[3] Materials Science Institute of Aragon (ICMA-CSIC) & Condensed Matter Physics, University of Zaragoza, 50009 Zaragoza, Spain

[4] IMDEA Nanoscience, Fco. Tomás y Valiente 7, 28049 Madrid, Spain

Abstract

We present here an study of historic glass decay by means of X-ray absorption spectroscopy (XAS). Transition metal cations incorporated in the glass as choromophores exhibit modifications of their oxidising state and chemical environment as the glass suffers a decay process. These modifications can be monitored by measuring x-ray absorption near edge structure, XANES, and extended x-ray absorption fine structure, EXAFS, spectra at the selected atomic species. We apply the technique here to glasses from different periods ranging form 1st century BC to 18th century, demonstrating that XAS provides an advanced tool for a quantitative analysis of glass decay. In particular we have found that it is possible to establish a relationship between the oxidation state of Fe and Cu cations with the decay suffered by the glass. In contrast, our results indicate that the Mn oxidizing state is not directly involved in the glass decay of the studied samples.

1. INTRODUCTION

Glasses have been produced and used in Europe since more than 2000 years and they have been found in excavations since Roman times. All glasses, regardless from their origin, suffer from decay phenomena which are strongly connected to their chemical composition [1,2] and to the surrounding environment. In general, corrosion of glasses is due to ions exchange on the surface. It begins with the hydration of the surface, followed by the ion exchange (H^+ from the environmental water by Na^+ and/or K^+ ions from the glass surface). A silica gel layer is then formed at the glass surface. If the environmental conditions remain unchanged, the alkalinity of the surface increases due to the presence of NaOH and/or KOH obtained as a reaction product. An alkaline attack begins at this step and produces the depolymerization of the three-dimensional silica network favouring the extraction of Ca, Mg, Al, and other ions that may react with pollutants and/or soil components. They develop corrosion salts in a more advanced step. The formation of these corrosion crusts complicate the analysis of historical glasses and the diagnosis of their decay [3,4].

The knowledge of the chemical composition, chromophores and surface structure is important for both archaeological glasses and glasses from stained

glass windows. It helps to complete historical knowledge, like provenance, dating and authentication studies; to optimize restoration and conservation procedures; and finally, to improve preservation strategies, like storage or exhibition conditions.

Chemical glass composition may range from soda-lime silicate to lead silicate or potash-lime, depending on their provenance and manufacture period. Within glass components, stand out glass chromophores or colouring agents, responsible of the glass colour. Glass colour is due to the oxidation state (OE) and electronic configuration of these chromophores. They are usually metal transition elements of the periodic table, which absorb characteristic frequencies of the visible region as a result of d-d or f-f electronic transitions [5]. They are normally added with the raw materials in very low concentrations. Main glass chromophores are transition metal ions, such as Fe^{2+}/Fe^{3+}, Co^{2+} or Mn^{3+}, or metal nanoparticles, such as Ag^0 or Cu^0.

There are few studies mentioning the importance of these elements (chromophores, pigments [6], etc.) in degradation processes, mainly because chromophores content is normally below the detection limit of conventional analytical techniques. However, they may be lixiviated like other components from the glass and remain in the degraded surface forming new salts with different environment and structure. Consequently, their characterization, mainly performed by using synchrotron x-ray radiation techniques [7], may offer new insights on the decay process of the glasses.

X-ray absorption spectroscopy (XAS) has proven to be an outstanding structural tool for studying the local geometric and electronic structure of matter [8]. Nowadays XAS is a widely-used technique in different scientific fields for determining the local environment (coordination numbers, chemical nature of bondings, symmetries, etc.) around a selected atomic species in a great variety of systems [9,10]. More recently, the increased accessibility of XAS user facilities along with improved X-ray optics, detectors, and user-friendly software has positioned XAS as an alternative tool to study cultural heritage materials due to their non-invasive and element specific character, low detection limits, high sensitivity and lateral resolution [11, 12, 13,14]. Although most of previous studies are focused on provenance and dating [15,16], the present research intends to illustrate the possibilities in the study of degradation processes of amorphous materials that can not be modified, like historical glasses are.

The purpose of the work is the study of historical original glass chromophores as indicators of their decay. We aim to establish a relationship between the oxidation state, the molecular environment and their degradation state by studying both the x-ray absorption near edge structure (XANES) and extended x-ray absorption fine structure (EXAFS) region at the selected atomic species.

3. MATERIALS AND METHODS

3.1 Historical Samples

All analyzed samples consisted in historical original glasses from different periods from the first century BC to the 18th century AC and different locations

inside Spain. They came from stained glass windows or from archaeological sites. Some of them showed heavily corrosion on their surfaces and some of them seemed not to be weathered (see Table 1). All the samples were coloured containing cooper, iron and/or manganese ions.

3.2 Analytical techniques

Surface morphology of the glasses was observed by optical microscopy with an Olympus BX60M optical microscope with reflecting light coupled to an Olympus DP11 camera and by scanning electron microscopy with a JEOL Scanning Microscope 6335 F working at 10.0 kV.

Transmission spectra of glasses were measured with a UV–VIS-NIR Shimadzu 3100 double-beam spectrophotometer equipped with an integrating sphere. Samples were placed behind a 1 mm width slit mask. Spectra were recorded from 200 to 800 nm with 0.5 nm spectral resolution.

XAS measurements were performed at the beamline BM25 (Spanish-SpLine) at the European Synchrotron Radiation Facility (ESRF). We measured X-ray absorption near edge structure (XANES) and extended x-ray absorption fine structure (EXAFS) spectroscopy at the Mn K-edge (6.5 keV), Fe K-edge (7.1 keV) and Cu K-edge (9.0 keV). Spectra were collected at room temperature in the fluorescence mode. Samples for were placed at 45º from incident X-rays and fluorescence signal was collected using a multi-element solid state detector. Four to seven scans of all samples were collected for signal averaging. The samples analyzed were those described in table 1. Additionally metallic Mn, Fe and Cu foils as well as their oxides were measured as reference compounds. The XAS spectra were analyzed according to standard procedures [5] using the ATHENA program pack.

4. RESULTS

4.1 Manganese containing glasses

Manganese is an element with OE from 0 to +7 and some Mn compounds can also show mixed valences. However, in glasses, Mn cations exhibit just valence +2 and +3. Mn^{3+} ions in silicate glasses are found only in octahedral environments (surrounded by 6 oxygen ions) while Mn^{2+} can be found in tetrahedral (4), penta-coordinated (5) or octahedral (6) environments. Since some centuries ago, Mn ions have been intentionally added to the raw materials for glass manufacture as decolorant or decolouring agent. The simultaneous presence of Mn and Fe ions leads to the oxidation of Fe^{2+} (blue-green) to Fe^{3+} (yellow) while Mn^{3+} (purple) is reduced to Mn^{2+} (lightly yellow), thus producing a color compensation [17].

Figure 1 a and b shows the Mn K-edge XANES spectra of the glass samples and the reference compounds [18]. Spectra recorded at various regions of different samples resulted identical within the experimental error, confirming that the glasses are very homogenous. The absorption edge of all glass samples is located at energies between the absorption edges of MnO and Mn_2O_3 reference compounds, being closer to that of MnO. Very often, displacements of the edge position are associated to changes in the oxidation state, according to the Kunzl law [19,20]. However, special caution has to be given to this direct assignment, i.e.

to relate the valence with the ''edge position'' because both the edge position and the overall spectral shape are intimately linked to the local structure of the absorbing atom [21,22,23]. Therefore, examination of the Mn K-edge position is a first qualitative indicator of the valence of manganese (keeping in mind this measurement is not quantitative). The edge energy of both reference compounds and samples has been defined as the inflection point of the XANES spectrum. As shown in Figure 2, the comparison of the Mn absorption edge energy versus the OE of the samples indicates that all glasses contain Mn ions mainly in a 2^+ oxidation state. In addition, the XANES spectra of all samples are similar showing a single-frequency oscillation, characteristic of highly disordered compounds. The low signal to noise ratio (S/N) of the acquired spectra prevent us of performing a detailed EXAFS analysis. In spite of this limitation, the comparison of the EXAFS and its Fourier transform (FT) recorded at the same experimental conditions on both samples and reference compounds allows us to extract valuable information regarding the first coordination shells. In this way all the samples show a single peak in the FT corresponding to a Mn-O coordination with an interatomic distance of ~ 2.2 Å, i.e. as in the case of MnO. Moreover, despite all the samples show a high disorder around the absorbing Mn site, both To_5 and MI_3 samples exhibit higher local order, within the aforesaid S/N, than the other samples. A final discussion is deserved to the study of the pre-edge region of the spectra which is more adequate to identify not only the redox state but also the symmetry of ions present in the glasses. In our case, all the compounds show a well defined pre-edge feature which indicates a non-center symmetric structure around the Mn sites. This is in agreement with the EXAFS results which indicate a highly disordered Mn coordination. Thus, these results suggest that these historical glasses present Mn^{2+} as a major component in highly disordered non-centrosymmetric sites without a clear distinction with the degree of alteration of the glasses.

4.2 Iron containing glasses

Iron is usually introduced in glasses as an impurity of silica raw materials. Concentrations are typically below 1 wt. % but it can vary extensively. Typical Fe oxidation states in glasses are +2 and +3. Fe^{2+} ions result in VIS absorption bands at 440, 1100 and 2100 nm (blue-green color) and Fe^{3+} ions in absorption bands at 380, 420 and 440 nm (yellow color).

Figure 3a shows XANES spectra of Fe K-edge of reference compounds. The most obvious feature is that the main peak broadens and shifts to higher energy as the Fe-O bond length decreases, i.e. as the oxidation state of the iron oxide compound increases. In the case of both Fe_3O_4 (magnetite) and γ-Fe_2O_3 (maghemite), a well defined pre-peak is observed below the absorption edge, indicating the presence of Fe ions occupying tetrahedral sites in the crystal. Indeed, Fe ions occupy in these compounds both octahedral (O_h) and tetrahedral (T_d) sites, while only octahedral sites are allowed in the case of α-Fe_2O_3 (hematite) whose XANES spectrum does not display such a pre-peak [12,24,25]. In our case (Fig. 3b), all samples show this pre-peak, indicating the presence of Fe cations in a non center-symmetric positions. In contrast, the edge position varies through the series (figure 4): the edge position of the Vi_2 sample is close to that of FeO; that of Re_1, Mi_3 and To_5 samples lies in between those of Fe_3O_4 and γ-Fe_2O_3; while the edge of the Me_14 sample

coincides with that of γ-Fe_2O_3. Moreover, as in the case of the Mn K-edge, the EXAFS oscillations of the glass samples are strongly damped with respect to those of the reference compounds, indicating a high degree of structural disorder. These results reveal on the one hand the coexistence of both Fe^{2+} and Fe^{3+} electronic states in the samples as well as the variation of the Fe^{2+}/Fe^{3+} ratio through the series. As shown in Figure 4, the Fe K-edge XANES spectrum of the Vi_2 glass mainly corresponds to Fe^{2+}, whereas Fe^{3+} is the dominant iron cation in the case of the Me_14 sample. Indeed the XANES spectrum of Me_14 is similar to that of maghemite. In the case of glass samples Mi_3, Re_1 and To_5 the edge position and the spectral shape indicate a mixture of Fe^{2+} and Fe^{3+} ions as in the case of both Fe_3O_4 and γ-Fe_2O_3. It should be also noted that the energy position of the first oscillation minimum after the edge (~ 40 eV) shifts to lower energies as moving from γ-Fe_2O_3 to Fe_3O_4, i.e. as the Fe-O interatomic distance increases. Accordingly, it is possible to distinguish 2 groups in the original historical glasses. Re_1, Mi_3, To_5 and Me_14 samples can be identified as a mixture of disordered magnetite-maghemite in which the Fe^{2+}/Fe^{3+} varies: magnetite is dominant in the case of the non-degraded Re_1 sample whereas Fe^{3+}, maghemite-like, is dominant in Me_14. In contrast Fe^{2+} is dominant in the case of the non-degraded Vi_2 sample whose XANES spectrum suggests a mixture of both FeO and Fe_3O_4 oxides. These results suggest that Fe^{2+}, in a magnetite-like arrangement, is the dominant species in the non-degraded glasses, evolving towards higher oxidation states as the surfaces are degraded.

4.3 Copper containing glasses

The three original red glass fragments under consideration (Mi_3, To_5 and Vi_2) show diverse degree of deterioration (Fig. 5). Sample Mi-3 is heavily corroded showing by optical microscopy an iridescent surface with abundant interconnected craters. Sample To-5 is light degraded showing some pits homogeneous distributed on the surface, and sample Vi-2 shows an almost not altered surface.

Optical absorption spectra of red glass samples show an absorption edge around 600 nm followed by a maximum at 570 nm defined only for thin red layers (Vi-2 and Mi-3) (Fig. 6a). This peak is attributed to inter-band transitions due to resonance of superficial Cu^0 plasmons [26], or Cu_2O nanoparticles above 20 nm size [27]. CuO nanoparticles present an increasing absorption profile in the 300-800 nm range, which could be also found in these samples [28],[29]. Despite the similar behavior of red glasses under VIS light, the XANES spectra show important differences when they are compared to the references (Fig. 7 a and b). In particular, sample Vi_2 shows a XANES spectrum similar to the Cu foil reference, indicating the presence of metal (Cu^0) nanoparticles, while those of Mi_3 and To_5 exhibit the characteristic edge resonance of Cu^{1+} in Cu_2O. These results are confirmed by the EXAFS analysis. The k-squared EXAFS spectra and their Fourier transforms (obtained using a Hanning window in the range $2 \leq k \leq 10$ $Å^{-1}$) reported in Figure 8 evidences that while Cu-Cu coordination is dominant in the Vi-2 sample, Cu-O coordination dominates the EXAFS spectra in the case of both Mi_3 and To_5 samples. Moreover, the analysis of both XANES and EXAFS spectra indicates that the dominant copper oxide in the samples is Cu_2O and not CuO, i.e. that the oxidation state of Cu is

essentially Cu^{1+} in all the studied samples with the exception of the metallic-like Vi_2. In addition, the EXAFS spectra of all the samples are characteristic of highly disordered systems in such a way that only a first oxygen coordination shell around the absorbing Cu is observed. The broadening of the FTs peak indicates a different degree of disorder in the samples. Regarding the red glass samples the Cu-O arrangement is more ordered and similar to the Cu_2O case for To_5 than for Mi_3. In the latter case, the lower intensity and greater broadening of the first shell peak in the FT indicates the spreading of Cu-O interatomic distances in a highly disordered Cu environment. These results are in agreement with the analysis of the XANES spectra performed by fitting the experimental spectra to the weighted sum of the XANES spectra of reference compounds. Indeed good reproduction of the experimental spectrum of the To_5 glass sample is obtained by considering the presence of 90% of Cu^+ (Cu_2O) and 10% of metallic Cu, while in the case of the Mi_3 glass one the best fit is obtained by considering a 10% of CuO (Cu^{2+}) in addition to a 90% of Cu^+ (Cu_2O).

Additionally, the EXAFS spectra indicate that the Vi_2 sample show well ordered metallic Cu regions. In contrast, the rest of the glass samples show a highly disordered Cu-O arrangement that is similar to that of Cu_2O for Le_13, To_5 and Le_19 samples. Both Re_1 and Mi_3 samples show the highest disordered with a spreading of the Cu-O interatomic distances that suggest also the presence of CuO and non-stoichiometric copper oxides (Fig. 8).

Optical absorption of green glass sample Me_14 shows an intense absorption band with a maximum intensity at around 780 nm, characteristic of Cu^{2+} ions. Glass Re_1, also showing green colour, shows two absorption bands, one at around 448.5 and a second one at 656.6 nm (Fig. 6b). The addition of network modifiers to the glass, like lead ions, shifts the absorption bands. In this glass, the UV-VIS absorption band appears at higher wavelengths than 400 nm and the second band appears exhibits a maximum at about 780-800 nm. In the case of glass Le_13, its blue colour together with the absorption bands that appears at 535 and 653 nm and the shoulder at 600 nm indicates the presence of Co^{2+} ions. These ions may avoid the absorption band due to Cu^{2+}, not appreciable by UV-VIS spectroscopy.

Sample Me_14 presents a detachment on the exterior side with a non-degraded surface (points 1 and 2), and a gel layer with an iridescent surface (points 4 and 5). In order to ascertain the decay degree of the surface successive XANES (Fig. 9) and EXAFS spectra (Fig. 10 a and b) were recorded at the different areas with a spot size of 0.5x1.0 mm. All the XANES spectra show an intense peak at the edge, characteristic of Cu^+ in Cu_2O as well as single oscillation spectral shape, indicative of highly disordered systems. This is evidenced in the comparison of the EXAFS spectra and their Fourier transforms reported in Figure 10 b. In all the cases a single peak is observed in the FT, which indicates that the Cu-O coordination extends only to the first neighbouring shell, being the interatomic Cu-O distance that found for Cu_2O. In addition, the amplitude of the EXAFS signal evolves differently through the five studied zones. The results indicate that the local order around Cu is higher in zones 1 and 2 than in the rest of the sample, in agreement with the evolution of the degradation through

the sample. This conclusion is also supported by the observed modification of the edge position. As shown in Figure 9, the edge position is the same (Cu^+ as in Cu_2O) for the spectra recorded in zones 1 and 2, i.e. in the (non-corroded areas), while it shifts towards higher energies in the other areas, indicating the increasing presence of Cu ions in a higher oxidation state in the degraded areas of the glass surface (points 3, 4 and 5). Finally, comparing areas from different samples (Fig. 11), it is possible to separate the red almost non-corroded glass from the rest, due to the abundance of Cu^0 colloids. Corroded red glasses, green and blue ones have both Cu ions in oxidation states +1 and +2 and the relation between both may indicate its degradation degree.

CONCLUSSIONS

According to the Cu K-edge absorption energy of red glasses Vi_2, To_5 and Mi_3 it is possible to establish a correlation between the OE and their surface decay, from non-weathered to middle and heavily corroded. Even on different areas of the same sample, as in Me_14 glass, it is possible to distinguish the non-corroded from the corroded areas. Additionally, Fe K-edge absorption XANES spectra of non-degraded glasses is located at lower energies than the ones for degraded ones, thus resulting in the possibility to discriminate weathered from non-weathered glass surfaces. Same results for Mn containing glasses are not so straightforward.

Taking into account the heterogeneous surface of historical original glasses and the presence of different degrees of alteration on the same glass (e.g. pits or corrosion crusts), all these results clearly show that it is possible to characterize the weathering phenomena of historical glasses from macroscopic to atomic scale in a totally non-degraded and non-invasive way.

ACKNOWLEDGEMENTS

The authors acknowledge the estimate help and comments of Prof. J. Llopis and Prof. M.A. Villegas. The Spanish Ministry of Economy and Competitiveness and Consejo Superior de Investigaciones Científicas is acknowledged for the financial support and for provision of synchrotron radiation facilities and the BM25-Spline staff for the technical support. This work has been supported by the Spanish Ministry of Economy and Competitiveness through the projects FIS-2008-06249, S2009-MAT-1629 (Geo-materials Program) and MAT2011-27573-C04-04, and by the Comunidad de Madrid NANOBIOMAGNET project and by the Aragón DGA NETOSHIMA grant. NC acknowledged the financial support of the FSE-MEC Ramón y Cajal program ref. RYC-2007-01715. MA and AS acknowledge the UCM Campus of International Excellence (PICATA Program) and the CSIC (JAE Program) respectively, for pre-doctoral fellowships.

TABLES AND FIGURE CAPTIONS

Table 1. samples description

Sample	Colour	Main colouring ion	Date	Provenance	Weathered (*)
Me-14	green	Cu^{2+}	1st C. BC	Archaeological site of Mérida	intermediate
Le-13	blue	Co^{2+}	13-14th C.	León cathedral	almost not
Le-19	blue	Co^{2+}	13-14th C.	León cathedral	heavily
To-5	red	Cu^{0}	15th C.	Toledo cathedral	intermediate
Mi-3	red	Cu^{0}	15th C.	Miraflores chartreuse	heavily
Vi-2	red	Cu^{0}	18th C.	Spanish stained glass windows	almost not
Re-1	green	Cu^{2+}	18th C.	Spanish stained glass windows	almost not

(*) considering the heterogeneous degree of alteration inside the same glass fragment.

Fig. 1 Normalized Mn K-edge XANES spectra of: a) reference compounds and sample Mi-3, and b) all original historical glasses.

Fig. 2 Relationship between Mn K-edge absorption energy and Mn oxidation state for samples (black circles) and references compound (red squares). The line is a linear fit for the reference compounds.

Fig. 3 Normalized Fe K-edge XANES spectra of: a) reference compounds and sample To_5, and b) all original historical glasses.

Fig. 4 Relationship between Fe K-edge absorption edge energy and Fe oxidation state for samples (black circles) and references compound (red squares). The line is a linear fit for the reference compounds (u-unweathered, w-weathered).

Fig. 5 Optical microscope images of the superficial features of glasses: a) Mi-3, b) To-5 and c) Vi-2.

Fig. 6 VIS absorption spectra of: a) red glasses Mi-3, To-5 and Vi-2; and b) green glasses Me-14 and Re-1 and blue glass Le-13.

Fig. 7 Normalized Cu K-edge XANES spectra of: a) reference compounds: metallic Cu, Cu_2O and CuO; and b) original historical red glasses: Mi-3, To-5 and Vi-2.

Fig. 8 Comparison of the Cu K-edge $k^2\chi(k)$ EXAFS signals and their Fourier Transform for both Cu references and glass samples.

Fig. 9 Comparison of different areas of sample Me_14 of the normalized Cu K-edge XANES spectra.

Fig. 10 Comparison of the Cu K-edge $k^2\chi(k)$ EXAFS signals (a) and their Fourier Transforms (b) for sample Me_14.

Fig. 11 Relationship between Cu K-edge absorption edge energy and Cu oxidation state a) reference compounds and different regions of sample Me_14 and b) reference compound and all the samples (black circles) and references compound (red squares). The line is a linear fit for the reference compounds (u-unweathered and w-weathered).

REFERENCES

[1] Roemich, H. Historic Glass and its interaction with the environment, In *The conservation of Glass and Ceramics*, edited by N. Tennent, London, James & James, 1999, pp. 5-14.

[2] García-Heras, M.; Gil, C.; Carmona, N.; Villegas M.A. *Mater. Construcc.* 2003, 53, 21-34.

[3] Carmona, N.; Villegas, M. A.; Fernández Navarro, J. M. *J. Eur. Ceram. Soc.* 2005, 25, 903-910.

[4] Roemich, H. Laboratory experiments to simulate corrosion on stained glass windows, In *The conservation of Glass and Ceramics*, edited by N. Tennent, London, James & James, 1999, 57-65.

[5] Weyl, W.A. Coloured glasses, In *Society of Glass Technology* Ed., United Kingdom, 1999.

[6] Bertrand, L.; Robinet, L.; Thoury, M.; Janssens, K.; Cohen, S.X.; Schöder, S. *Appl. Phys. A.*2012, 106, 377-396.

[7] Bertrand, L.; Cotte, M.; Stampanoni, M.; Thoury, M.; Marone, F.; Schöder, S. *Physics Reports* 2012, 519, 51-96.

[8] Sayers, D. E.; Bunker, B. A. In X-Ray Absorption: Principles, Applications, Techniques of EXAFS, SEXAFS, and XANES, D. C. Koningsberger and R. Prins Eds., Wiley, New York, 1988, chapter 6.

[9] Harbottle, G. *Nuclear Instruments and Methods in Physics Research B* 1986, 14, 10-15.

[10] Cartechini, L.; Miliani, C.; Brunetti, B.G.; Sgamellotti, A.; Altavilla, C.; Ciliberto, E.; D'Acapito, F. *Appl. Phys. A* 2008, 92, 243-250.

[11] Grolimund, D.; Senn, M.; Trottmann, M.; Janousch, M.; Bonhoure, I.; Scheidegger, A.M.; Markus, M. *Spectrochimica Acta Part B* 2004, 59, 1627-1635.

[12] Gautier-Soyer, M. *J. Eur. Ceram. Soc.* 1998, 18, 2253-2261.

[13] Dik, J.; Janssens, K.; Van Der Snickt, G.; Van der Loeff, L.; Rickers, K.; Cotte, M.; *Anal. Chem.* 2008, 80, 6436-6442.

[14] Cotte, M.; Susini, J.; Dik, J.; Janssens, K. *Acc. on Chem. Res.* 2010, 43, 705-714.

[15] Lahlil, S.; Cotte, M.; Biron, I.; Szlachetko, J.; Menguy, N.; Susini, J. *J. Anal. At. Spectrom.* 2011, 26, 1040-1050.

[16] Barilaro, D.; Crupi, V.; Majolino, D.; Venuti, V.; Barone, G.; D'Acapito, F.; Bardelli, F.; Giannici, F. *J. of Appl. Phys.* 2007, 101, 064909.

[17] Fernández Navarro, J.M. El vidrio, In Consejo Superior de Investigaciones Cientificas Ed., Spain, 2003.

[18] Farges, F. *Physical Review* B 2005, 71, 155109 1-14.

[19] Kunzl, V. *Collect. Trav. Chim. Techecolovaquie* 1932, 4, 213.

[20] Nedoseykina, T.; Gyu Kim, M.; Park, Seul-A.; Kim, Hyun-Soo; Kim, Seong-Bae; Cho, J.; Lee, Y. *Electrochimica Acta* 2010, 55, 8876-8882.

[21] Chalmin, E.; Farges, F.; Brown Jr, G. E. *Contrib Mineral Petrol* 2009, 157, 111–126.

[22] Farges, F. *Phys Chem Minerals* 2009, 36, 463–481.

[23] Chaboy, J. *J. Synchr. Rad.* 2009, 16, 533—544.

[24] Wilke, M.; Farges, F.; Petit, P.M.; Brown, G.E.; Martin, F. *American Mineralogist* 2001, 86, 714-730.

[25] Quartieri, S.; Riccardi, M.P.; Messiga, B.; Boscherini, F.; *J. Non-Crystalline Solids* 2005, 351, 3013-3022.

[26] Pedersen, D.B.; Wang, S. *J. Phys. Chem. C* 2007, 111, 17493-17499.

[27] Borgohain, K.; Murase, M.; Mahamuni, S.; *J. Appl. Phys.* 2002, 92-3, 1292-1297.

[28] Zhang, X.; Zhang, D.; Ni, X.; Zheng, H.; *Solid-State Electronics* 2008, 52, 245-248.

[29] Wang, H.; Xu, J.-Z.; Zhu, J.-J.; Chen, H.-Y.; *Journal of Crystal Growth* 2002, 244, 88-94.

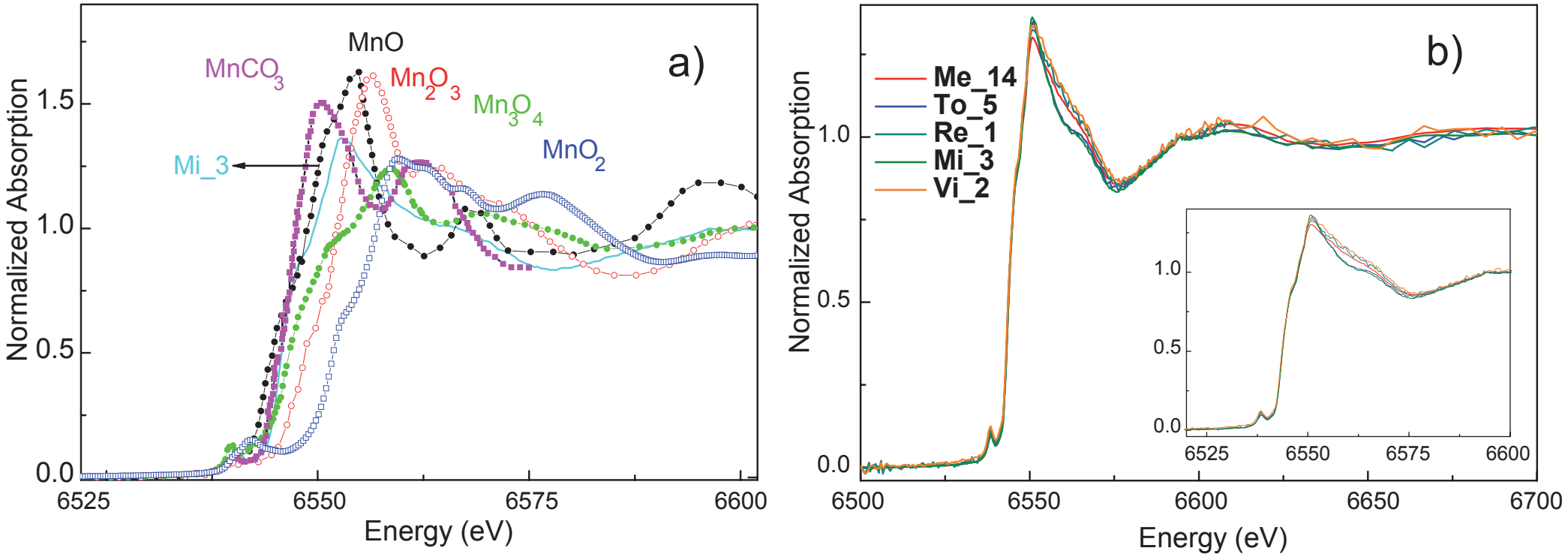
a)
MnO
MnCO3
Mn2O3
Mn3O4
MnO2
Mi_3
Normalized Absorption
Energy (eV)
b)
Me_14
To_5
Re_1
Mi_3
Vi_2
Normalized Absorption
Energy (eV)

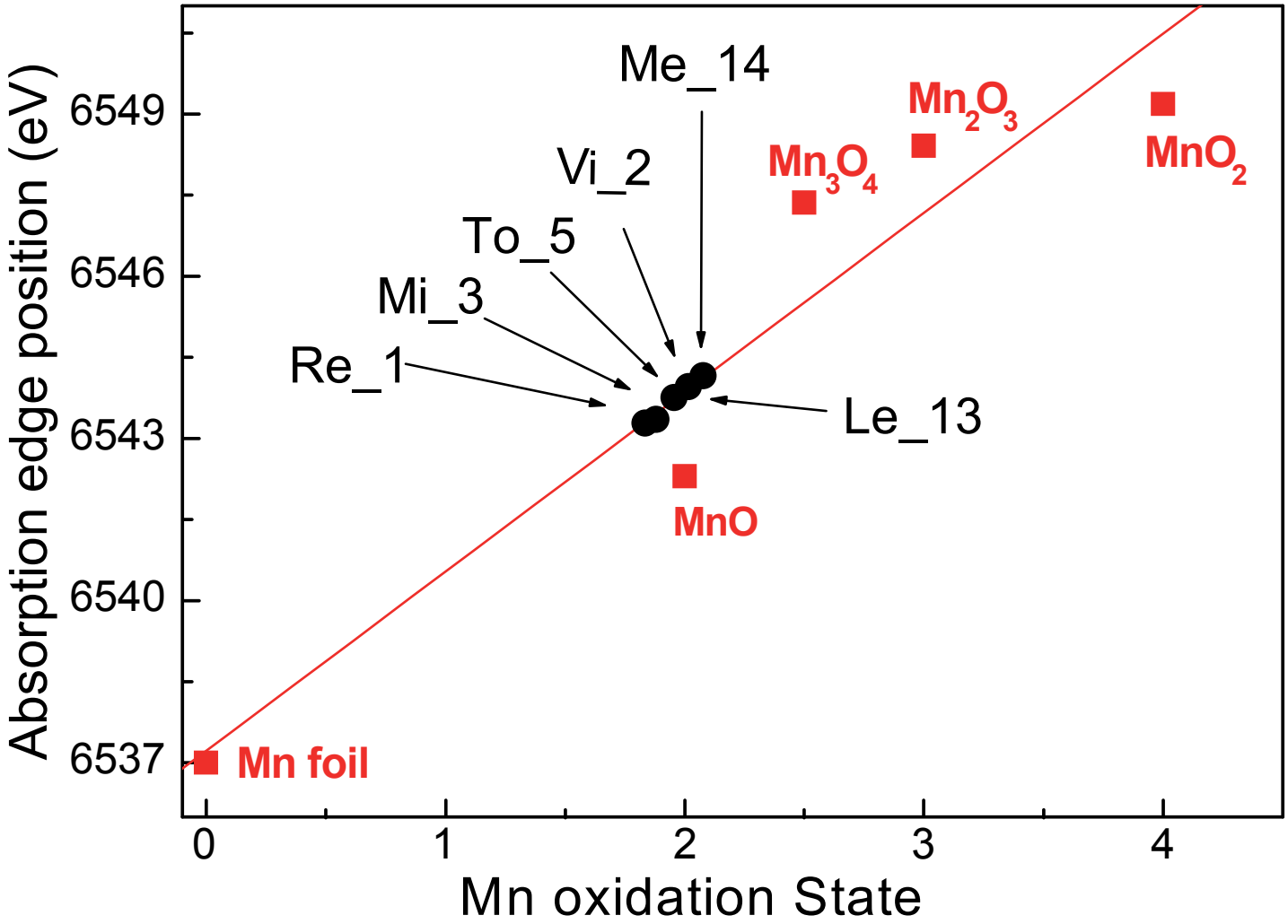
Absorption edge position (eV)
6549
6546
6543
6540
6537
0
1
2
3
4
Mn oxidation State
Me_14
Vi_2
To_5
Mi_3
Re_1
Le_13
Mn foil
MnO
Mn3O4
Mn2O3
MnO2

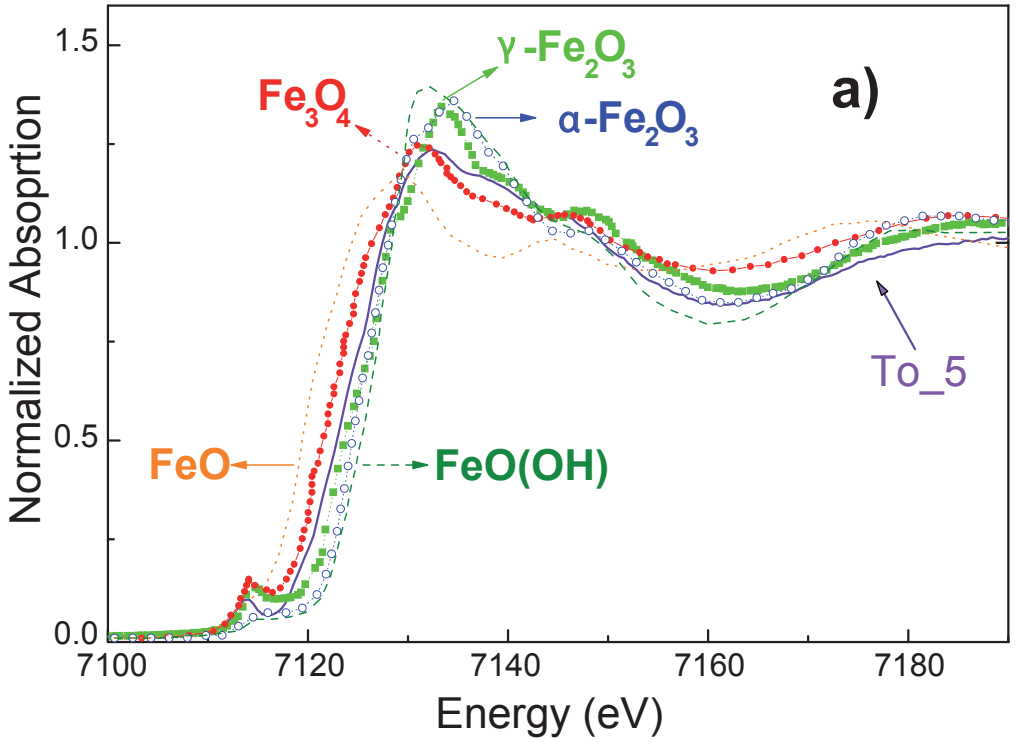
a)
Fe3O4
γ-Fe2O3
α-Fe2O3
FeO
FeO(OH)
To_5
Normalized Absoprtion
Energy (eV)
1.5
1.0
0.5
0.0
7100
7120
7140
7160
7180

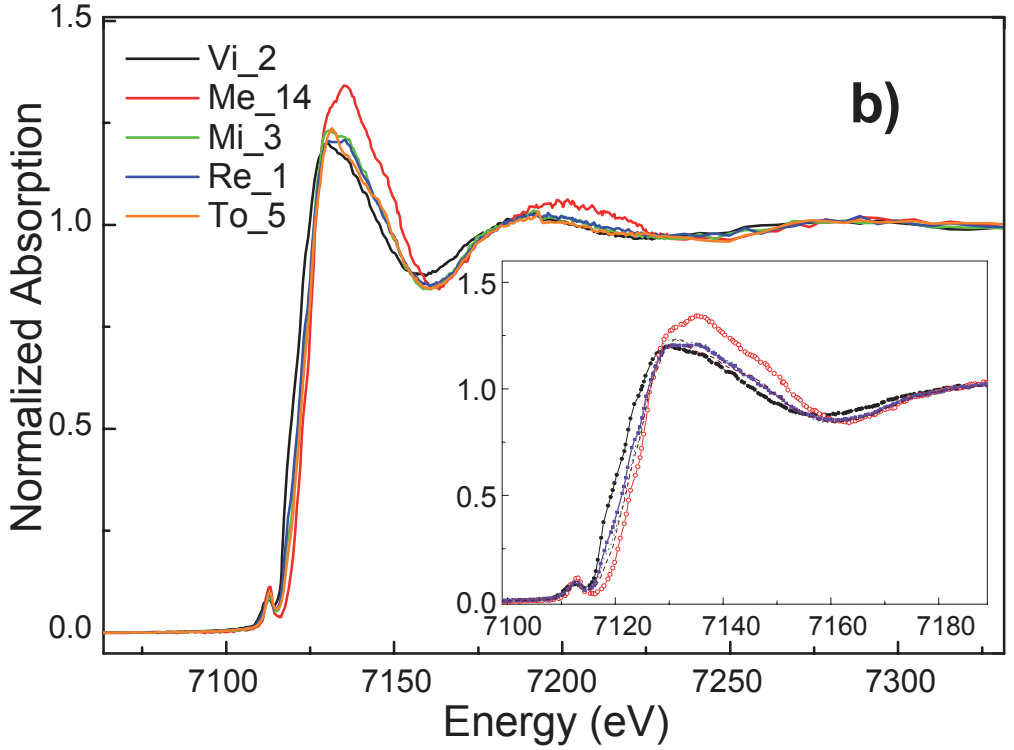
b)
Vi_2
Me_14
Mi_3
Re_1
To_5
Normalized Absorption
Energy (eV)
1.5
1.0
0.5
0.0
7100
7150
7200
7250
7300
7120
7140
7160
7180

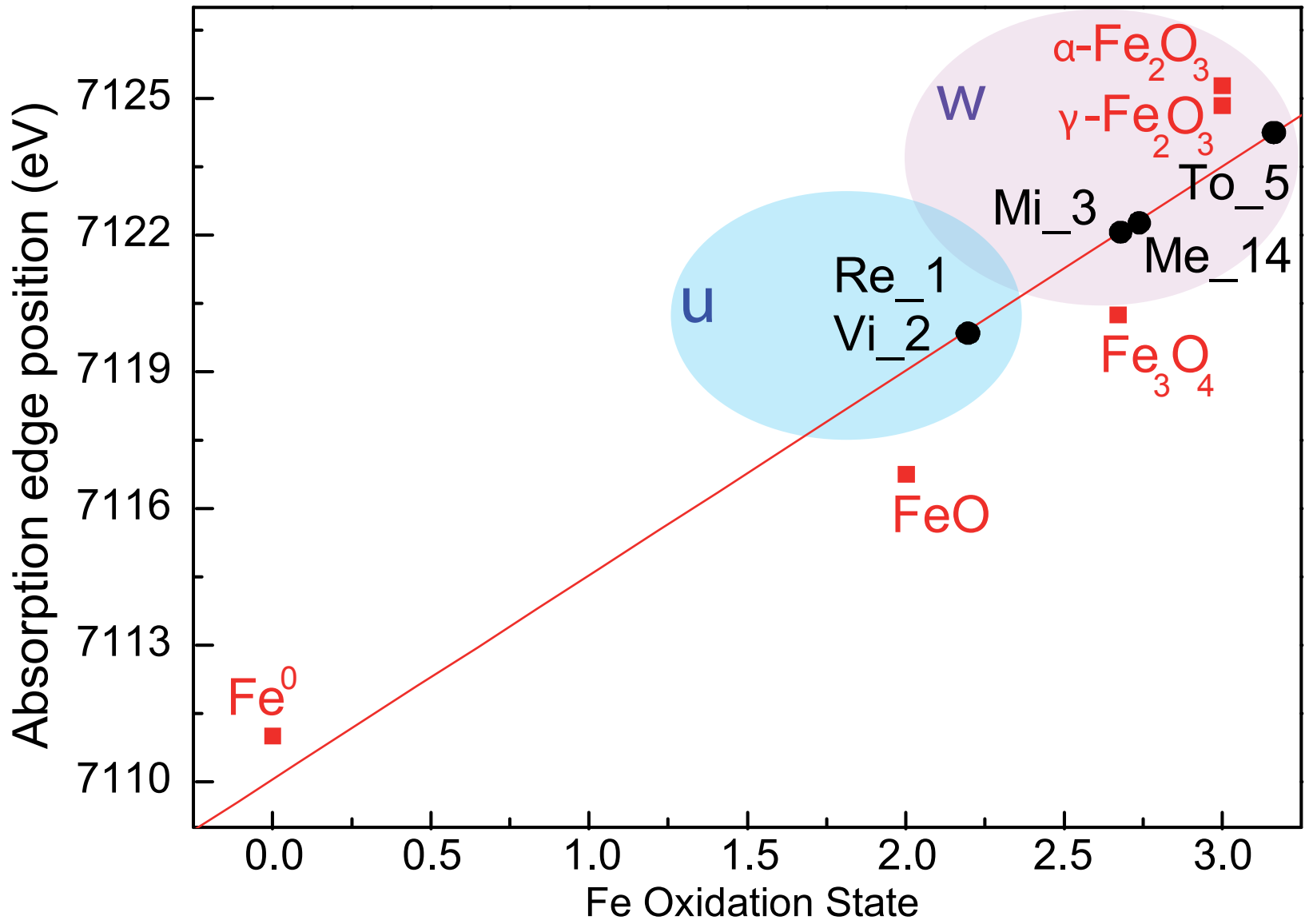
Absorption edge position (eV)
7125
7122
7119
7116
7113
7110
0.0
0.5
1.0
1.5
2.0
2.5
3.0
Fe Oxidation State
α-Fe2O3
γ-Fe2O3
w
To_5
Mi_3
Me_14
u
Re_1
Vi_2
Fe3O4
FeO
Fe0

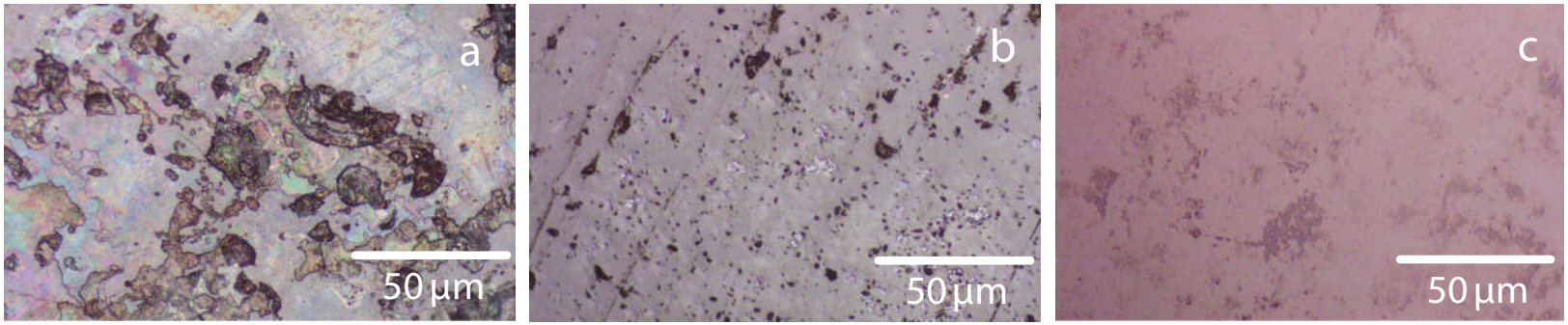
a
50 µm
b
50 µm
c
50 µm

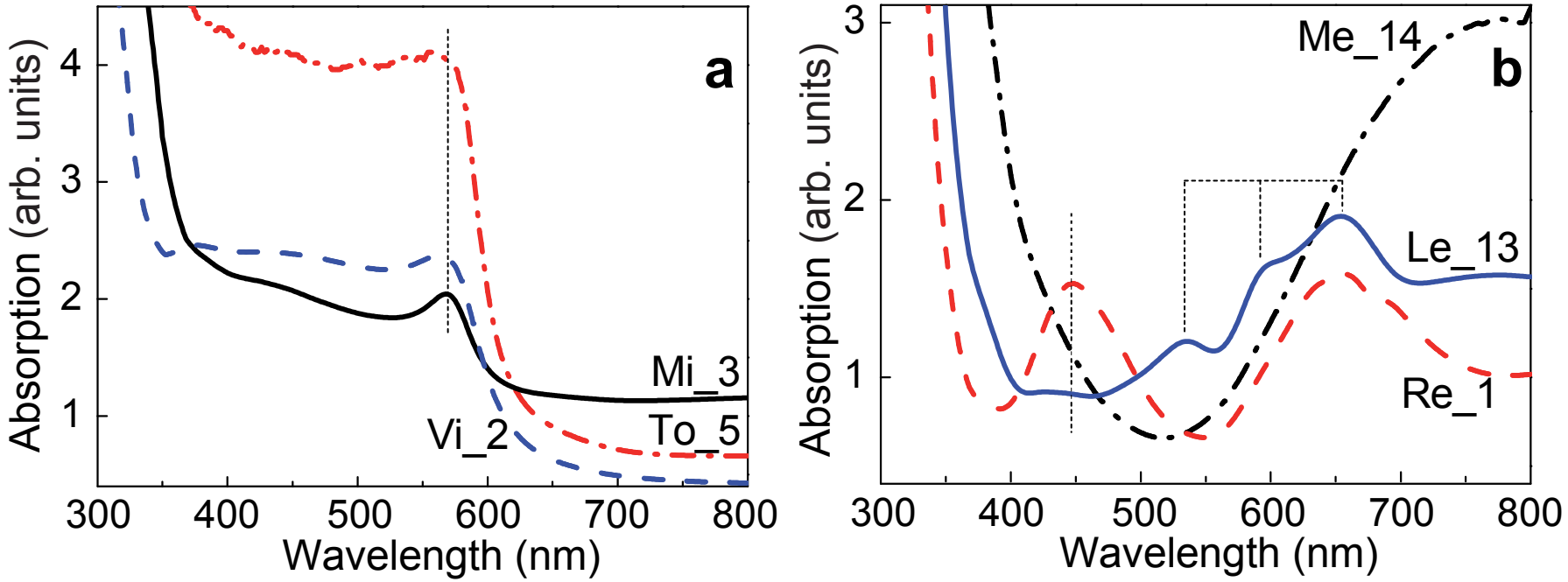
a
Absorption (arb. units)
Wavelength (nm)
Mi_3
Vi_2
To_5
b
Me_14
Le_13
Re_1

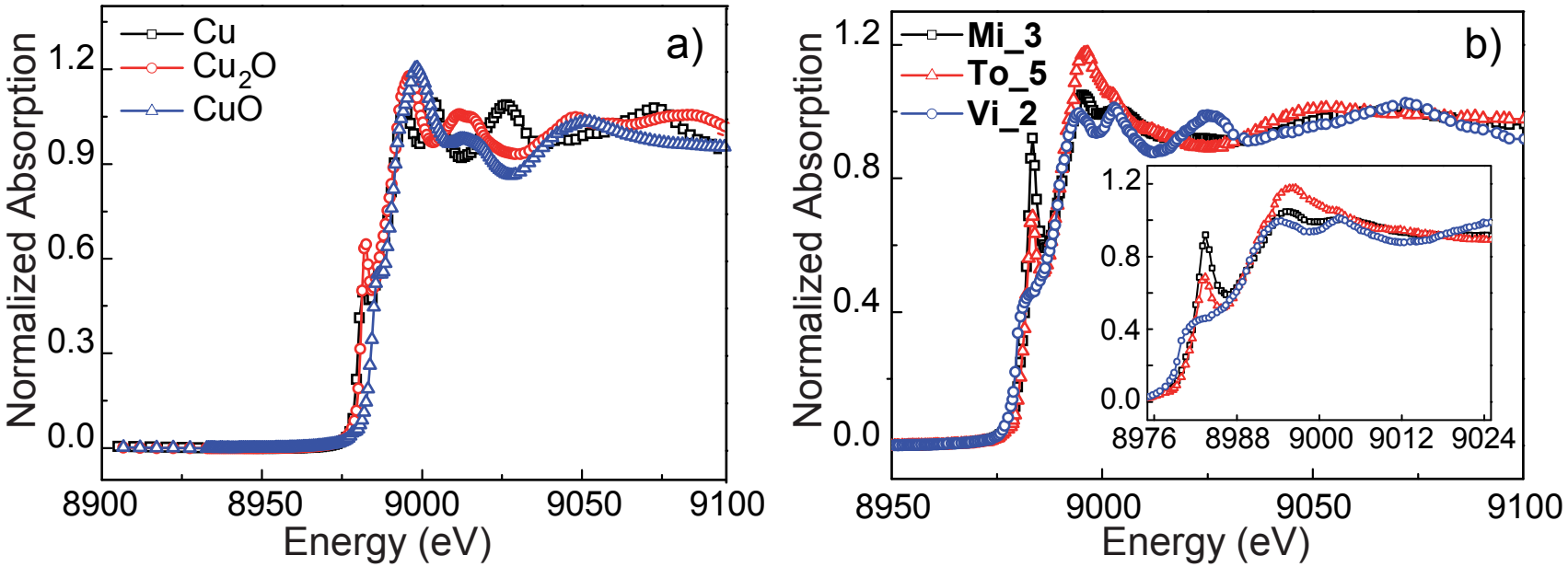
a)
Cu
Cu2O
CuO
Normalized Absorption
Energy (eV)
b)
Mi_3
To_5
Vi_2
Normalized Absorption
Energy (eV)

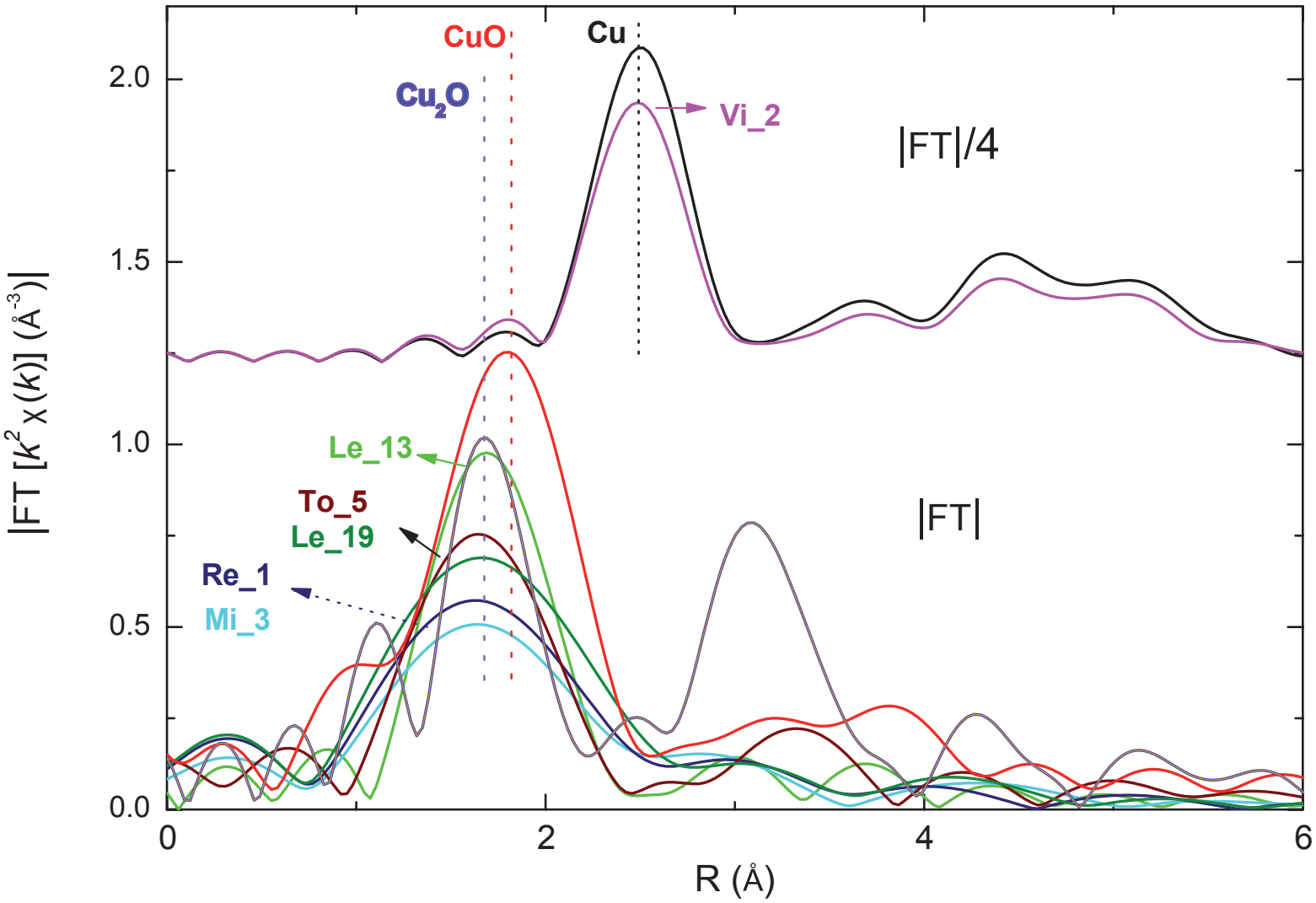
CuO
Cu
Cu2O
Vi_2
|FT|/4
Le_13
To_5
Le_19
Re_1
Mi_3
|FT|
|FT [k2 χ(k)] (Å-3)|
R (Å)
0.0
0.5
1.0
1.5
2.0
0
2
4
6

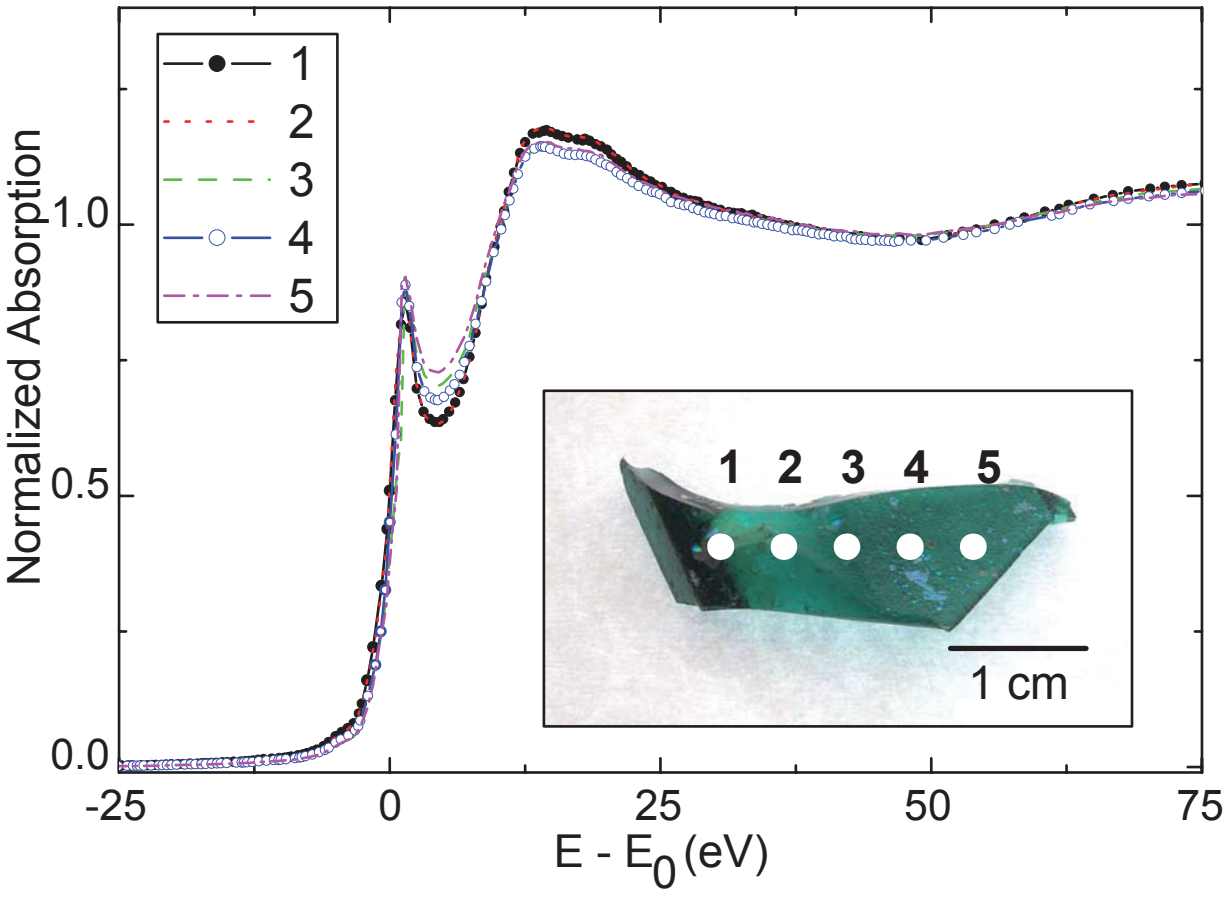
1
2
3
4
5
Normalized Absorption
0.0
0.5
1.0
-25
0
25
50
75
E - E0 (eV)
1 2 3 4 5
1 cm

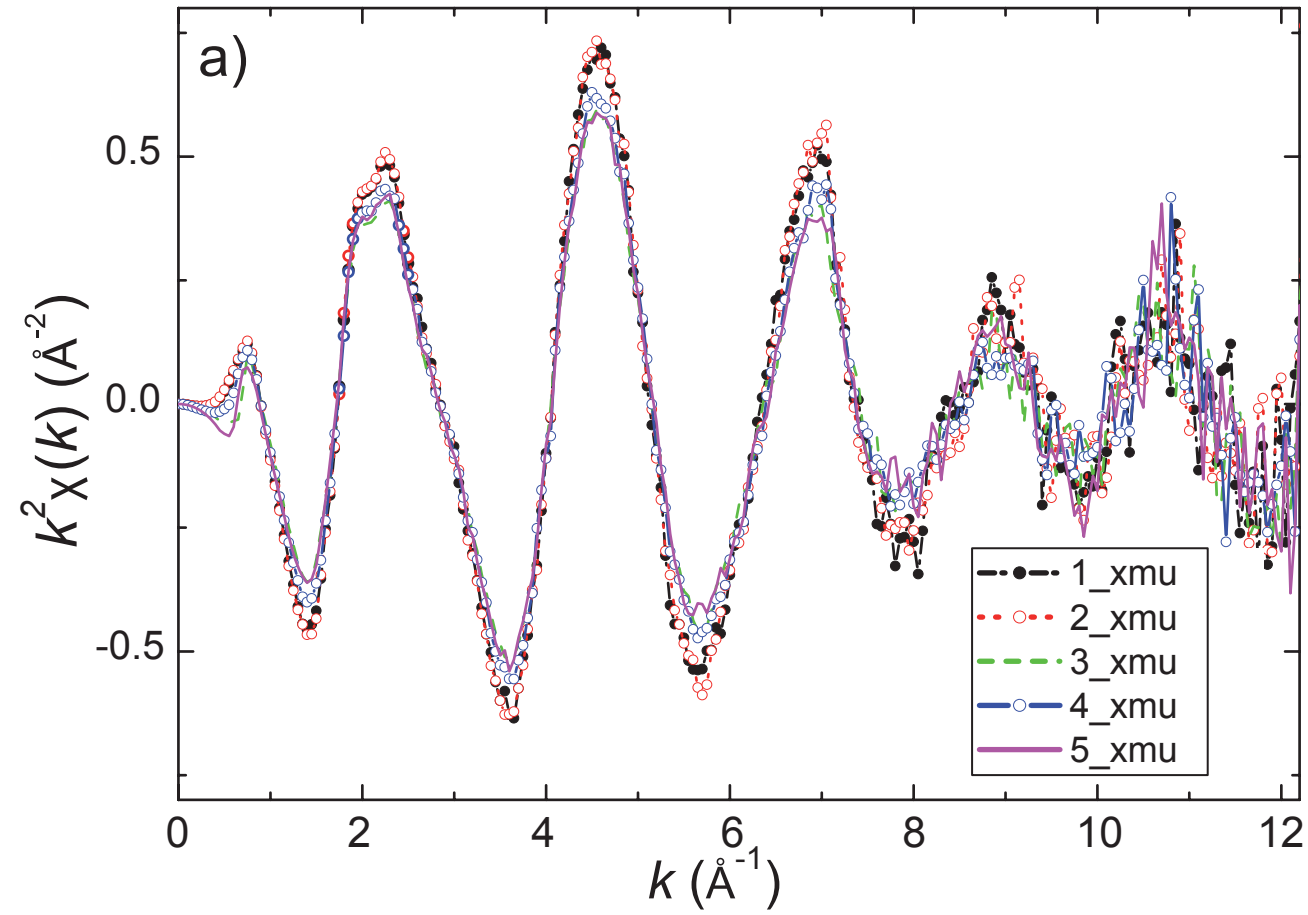
a)
0.5
0.0
-0.5
$k^2\chi(k)$ (Å^{-2})
0
2
4
6
8
10
12
k (Å^{-1})
1_xmu
2_xmu
3_xmu
4_xmu
5_xmu

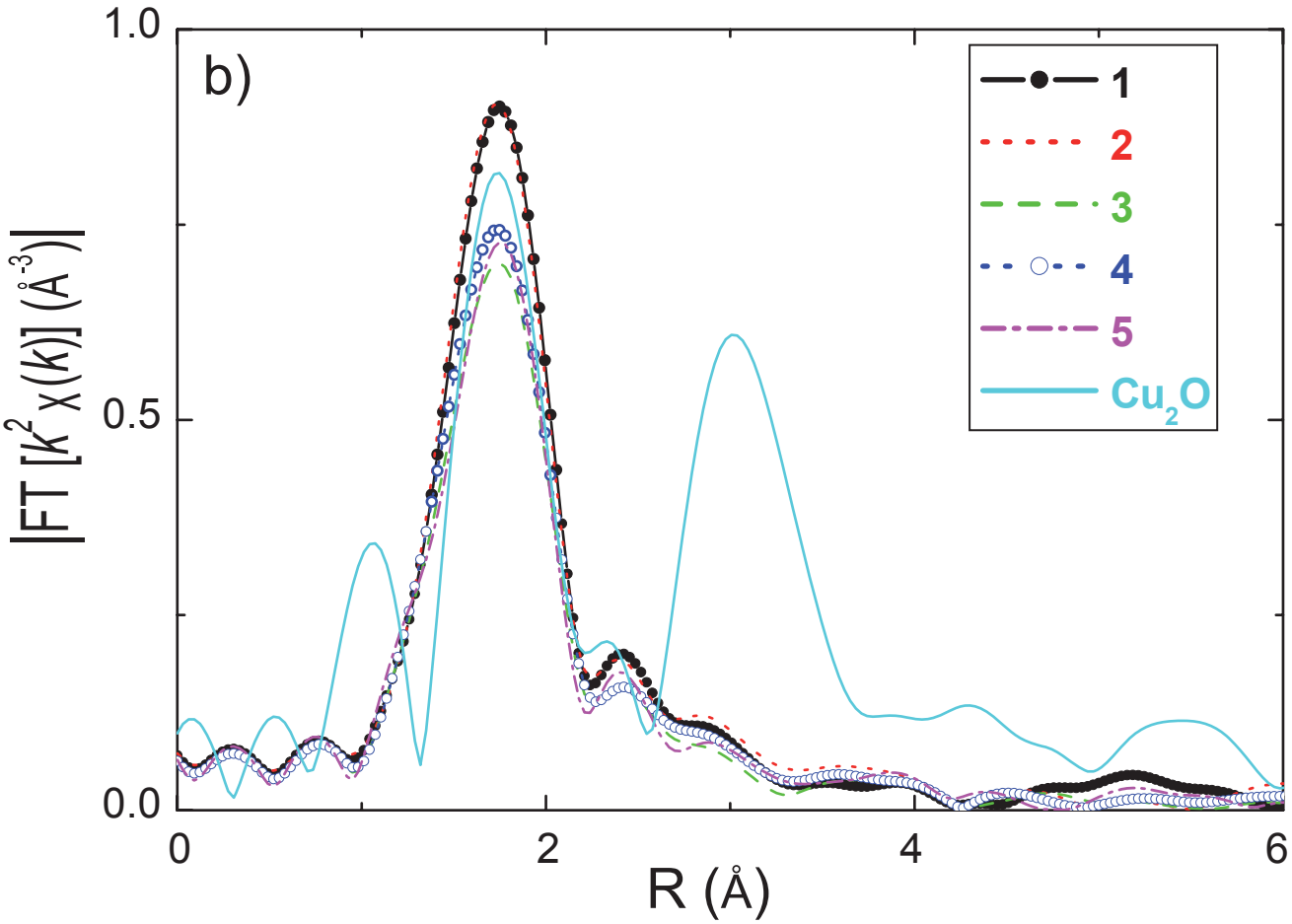
b)
1.0
0.5
0.0
|FT [$k^2\chi(k)$]| (Å^{-3})
0
2
4
6
R (Å)
1
2
3
4
5
Cu_2O

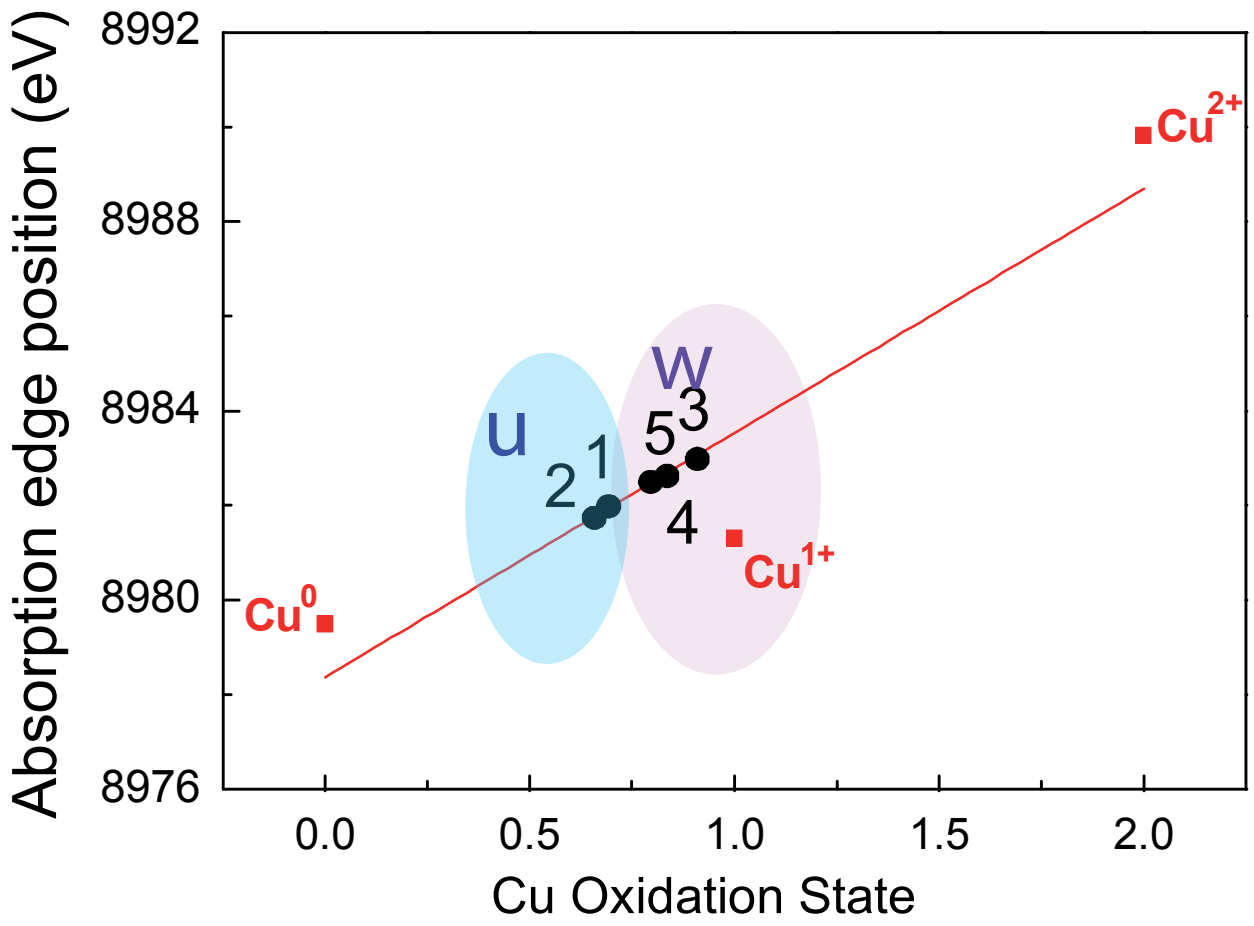
Absorption edge position (eV)
8992
8988
8984
8980
8976
0.0
0.5
1.0
1.5
2.0
Cu Oxidation State
Cu0
Cu1+
Cu2+
u
W
1
2
3
4
5

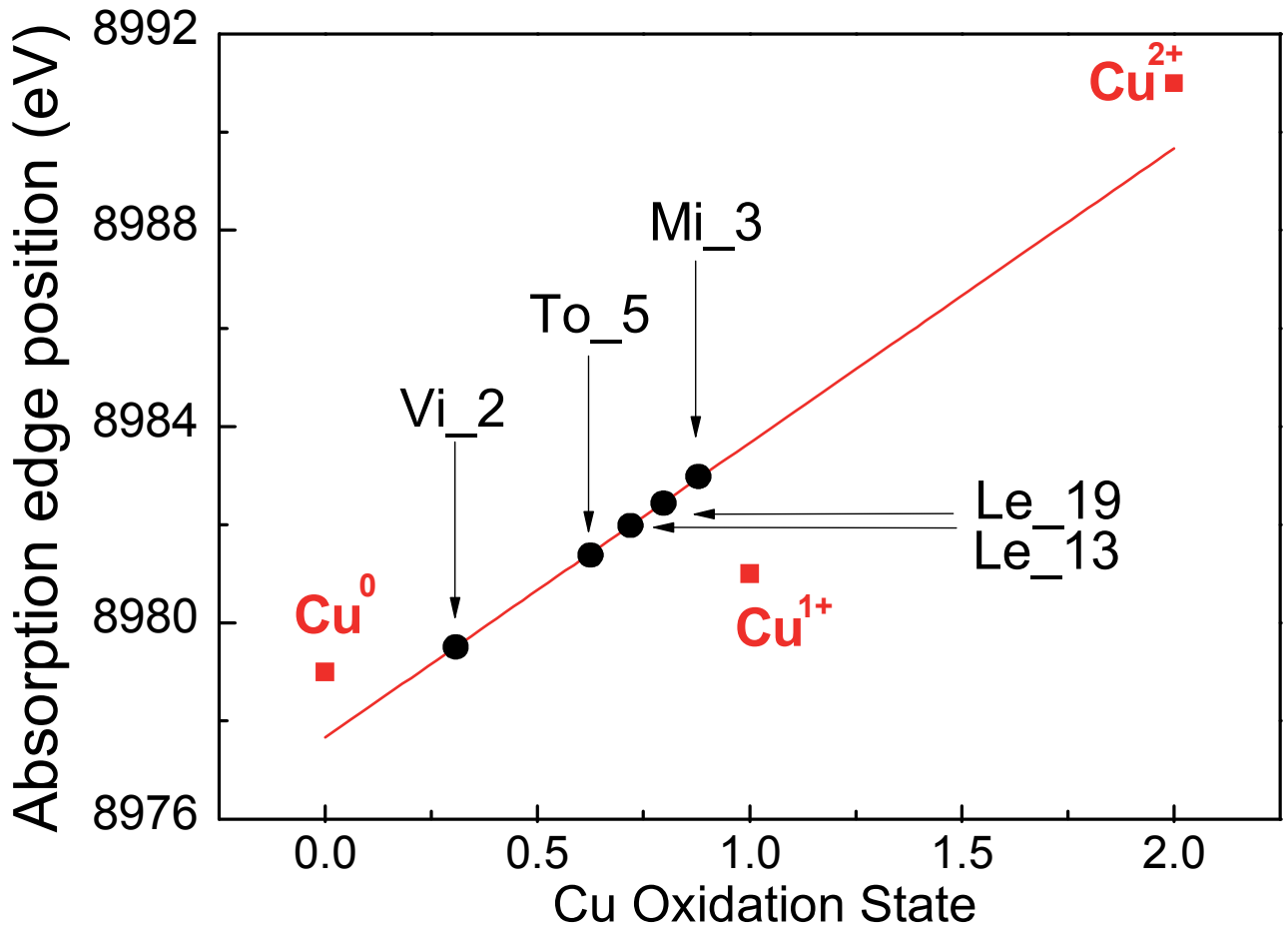
Absorption edge position (eV)
8992
8988
8984
8980
8976
0.0
0.5
1.0
1.5
2.0
Cu Oxidation State
Cu0
Cu1+
Cu2+
Vi_2
To_5
Mi_3
Le_19
Le_13